

# Performance of planar free-breathing PEMFC at temperatures below freezing

Tero Hottinen\*, Olli Himanen, Peter Lund

*Helsinki University of Technology, Laboratory of Advanced Energy Systems, P.O. BOX 2200, FIN-02015 TKK, Finland*

Received 25 January 2005; accepted 11 March 2005

Available online 31 May 2005

## Abstract

For practical fuel cell applications it is vital to know how the fuel cell operates in varying ambient conditions, especially when passive control methods are used. In this contribution, the effect of subzero temperatures with constant current density and cold-start behavior of planar free-breathing PEMFC were studied in a temperature chamber. The temperature levels used in constant current measurements varied between 0 and  $-27.5^{\circ}\text{C}$ . The cell maintained stable operation without irreversible performance losses at higher current densities as the heat generation was high enough to prevent the product water from freezing inside the cell. However, ice formation on the outer part of the cathode side of the cell was observed. At low temperature and current density level, the freezing of product water inside the cell led into irreversible performance loss. The cold-start measurements showed that the cell is capable of starting operation at  $-5^{\circ}\text{C}$  without irreversible performance losses when the cell is initially dry. The cell was capable of starting operation also at  $-10^{\circ}\text{C}$  when the starting procedure was slow enough, but a slight irreversible performance loss was encountered.

© 2005 Elsevier B.V. All rights reserved.

**Keywords:** PEMFC; Free-breathing; Freezing; Cold-start; Planar cell

## 1. Introduction

Polymer electrolyte membrane fuel cells (PEMFCs) are intended to be used as power sources in transportation, portable electronics and stationary applications. A power source of portable electronic device must have high energy density and it must be able to operate under varying ambient conditions. In small applications, the energy density may be increased with passive methods of operation as the number and power consumption of auxiliary devices is minimized. One interesting approach is to use a so-called free-breathing cell, i.e., a fuel cell that takes the oxygen needed in the reactions passively from ambient air. Because oxygen supply is passive in free-breathing fuel cells, it is important to know the effect of ambient conditions on the operation of the cell. The effect of ambient temperature and humidity on the operation of a free-breathing PEMFC have been reported e.g. in [1,2].

The power source of a portable electronic device must be able to operate and start also at temperatures below freezing point of water (subzero temperatures on Celsius scale). There are only a few published studies investigating the effect of cold temperatures on the operation of forced-convection PEMFCs and the authors are unaware of any published on free-breathing PEMFCs. Cho et al. [3,4] studied the effect of water removal on the performance of a PEMFC repetitively brought down to  $-10^{\circ}\text{C}$ . They concluded that the observed performance degradation can be reduced by removing the water from the cell by supplying dry gases or an antifreeze solution into the cell before the cell temperature fell below  $0^{\circ}\text{C}$ . Hishinuma et al. [5] studied the operation and cold-start behavior of a PEMFC at temperatures below  $0^{\circ}\text{C}$  by experiments and simulation. They concluded that the cell needs external heating in order to be able to start the operation at temperatures below  $-5^{\circ}\text{C}$ . Datta et al. [6] reported the experiences of successfully using a PEMFC system at the Indian Scientific Research Station in Antarctica at temperatures down to  $-40^{\circ}\text{C}$ .

\* Corresponding author. Tel.: +358 9 451 3209; fax: +358 9 451 3195.  
E-mail address: [tero.hottinen@tkk.fi](mailto:tero.hottinen@tkk.fi) (T. Hottinen).

In this paper the operation of a planar free-breathing PEMFC at temperatures below freezing point was studied using a temperature chamber. The operation of the cell was highly passive, only the hydrogen flow rate was controlled. The cell was started at room temperature and operated with constant current. When the temperatures and voltage of the cell were stabilized, the temperature chamber was set to a certain temperature level. Operation of the cell was studied at chamber temperatures between 0 and  $-27.5^{\circ}\text{C}$ . Cold-start behavior of the cell was also studied at chamber temperatures of  $-5$  and  $-10^{\circ}\text{C}$ . The cell was dried at room temperature, cooled down and then started with a certain procedure.

## 2. Experimental

The measurements were performed with a planar free-breathing PEMFC having an active area of approx.  $6\text{ cm}^2$ . The cell was operated in vertical cell orientation. The fuel cell components were the same as in [7] with a compressible carbon paper as cathode side gas diffusion backing (GDB) and cathode current collector having 2 mm wide openings. The measurements were conducted with the same measurement system as in [7,8] with the exception that the cell was placed inside a temperature chamber and the temperature of the cell was measured with two PT-100 Class-A temperature probes. The sensors were located on the surface of the cathode side of the cell; one was on the upper edge (temperature referred as  $T_1$  in the text) and the other on the lower edge ( $T_2$ ) of the cell. Temperatures were logged with Agilent 34901A 20 Channel Multiplexer connected to Agilent 34970A datalogger. The datalogger was controlled with HP Benchlink 1.1 program.

The temperature chamber was modified by the authors for laboratory use from EC1109N freezer made by Electrolux. The original temperature controller of the freezer was discarded and the chamber temperature was controlled with West 6100 controller. The lowest achievable temperature with the chamber was  $-27.5^{\circ}\text{C}$ . The temperature of the chamber was measured with two PT-100 Class-B probes. One probe was used by the temperature controller and the other was used for logging the chamber temperature ( $T_{\text{ch}}$ ). The measurement system was also equipped with a digital camera located inside the chamber. The camera was used to get visual information on ice formation on the open cathode structure of the cell.

A free-breathing fuel cell consumes oxygen from and produces water vapor into the surrounding air. If the fuel cell is operated inside a closed chamber without ventilation, the performance of the cell will eventually decrease because of decrease in oxygen partial pressure and increase in the humidity level of air. In addition, the more oxygen is consumed and water vapor produced, the more air is stratified, i.e. the humidity level rises more in the upper parts of the chamber than in the lower parts. In order to see if the chamber affects the cell performance, the cell was operated with the chamber cover closed for several hours with an average current density of

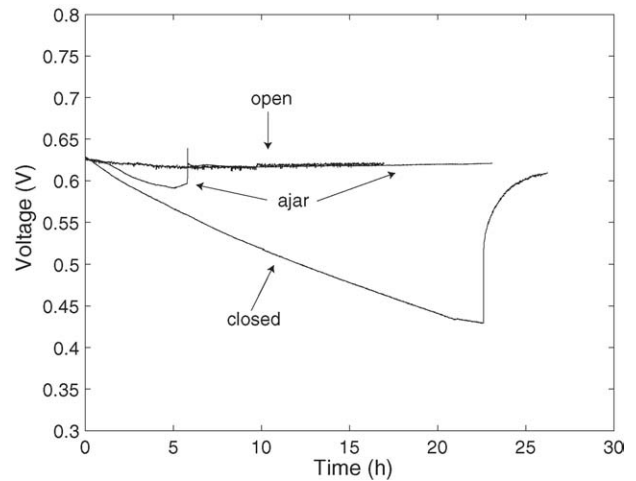


Fig. 1. The effect of temperature chamber ventilation on the cell operation. The position of the chamber cover is denoted with an arrow pointing to the corresponding curve.

$400\text{ mA cm}^{-2}$ . The temperature of the chamber in this measurement was approximately  $22\text{--}23^{\circ}\text{C}$ . Cell voltage from this measurement is illustrated in Fig. 1 as curve ‘closed’. The effect of improper chamber ventilation is evident as the cell voltage starts to decrease practically immediately when the chamber is closed. When the cover was opened after ca. 22.5 h, the cell voltage started to increase towards the initial level. The stratification of air was observed by measuring temperature and relative humidity of the chamber with Vaisala HMI41 relative humidity and temperature indicator with HMP42 probe. Before the cover was opened, the relative humidity and temperature in the upper part were 83.3% and  $23.0^{\circ}\text{C}$ , and 57.4% and  $22.9^{\circ}\text{C}$  in the lower part of the chamber.

Different chamber ventilation methods were investigated at room temperature in order to minimize the effect of air composition change and stratification. It was found that by feeding air into the bottom of the chamber with a flow-rate of  $400\text{ ml min}^{-1}$  and keeping the cover 5 mm ajar was enough to prevent the observed decrease in cell performance. Cell voltage from this measurement is illustrated in Fig. 1 as curve ‘ajar’. The airflow into the chamber was kept constant throughout the measurement and the cover, which was initially closed, was opened after 6 h and left ajar. This can be seen as a clear jump in voltage after which it stabilized. In order to assure that the airflow did not improve the cell performance by increasing the natural convection occurring on the surface of the cell, one measurement was conducted with the chamber open and without feeding air into the chamber. Cell voltage of this measurement is illustrated in Fig. 1 as curve ‘open’. The cell voltage remained stable and practically coincided with the voltage when the cover was ajar.

In all of the measurements, dry hydrogen having purity of 99.999% was fed to the anode. The hydrogen outlet was at ambient pressure, and thus the cell was not pressurized unless mentioned otherwise. The inlet pressure was measured with

Table 1

The chamber temperature ( $T_{\text{ch}}$ ) and current density ( $i$ ) levels used in the measurements with the corresponding temperature fluctuations ( $\Delta T_{\text{ch}}$ )

$T_{\text{ch}}$ (°C)	$i$ (mA cm <sup>-2</sup> )	$\Delta T_{\text{ch}}$ (°C)
0	200	±1
-5	200	±0.5
-10	200	±0.3
-10	300	±0.3
-15	300	±0.2
-15	400	±0.2
-20	500	±0.2
-27.5	600	±0.05

Brooks 5866 pressure controller. The minimum flow-rate of hydrogen was set to 7 ml min<sup>-1</sup> and for larger flows a current-based relation of 11 ml min<sup>-1</sup> A<sup>-1</sup> (stoichiometric ratio of 1.5) was used. Besides the hydrogen flow control, the cell was operated using passive methods, i.e. it had no external heating, it was fully free-breathing, and it did not have any active control on the water balance.

The effect of subzero temperatures on the cell performance was studied by measuring the cell voltage at constant current level. The cell resistance was simultaneously measured with current interruption method built-in to the measurement system. In these measurements the cell was first operated at room temperature with constant current, and after the cell voltage stabilized the temperature of the chamber was decreased to the desired temperature. The chamber temperature ( $T_{\text{ch}}$ ) and average current density ( $i$ ) levels used in the measurements are listed in Table 1 with the corresponding temperature fluctuations ( $\Delta T_{\text{ch}}$ ) after the chamber temperature stabilized.

The polarization curve of the cell was measured in ambient laboratory conditions between each of the temperature chamber measurements. This polarization curve was compared with a reference curve measured before the measurement series in order to reveal possible irreversible performance losses due to freezing of product water inside the cell. The polarization curves were measured by scanning the current with 100 mA steps and simultaneously measuring the cell voltage. The voltage was allowed to stabilize for 60 s at each measurement point before the next current step. Before each

polarization curve measurement, the cell was let to stabilize at the average current density of 100 mA cm<sup>-2</sup> for 15 min. In order to avoid the effect of load history, the polarization curve was measured three times in a row at 4 h intervals. The second and the third curves were practically coinciding in all of the measurements, and thus the third one was considered reliable in revealing the possible irreversible performance losses. If the comparison of polarization curves showed changes in the cell performance, the MEA and GDBs were replaced.

Cold-start measurements were performed at temperatures of -5 and -10 °C. Before decreasing the temperature of the chamber, the cathode of the cell was dried with an air pulse from a compressed air line and the anode was dried by flushing it with 100 ml min<sup>-1</sup> nitrogen until the cell voltage was decreased to zero. The cell was dried in order to prevent the freezing of water inside the cell as there was no heat production during the temperature decrease. The chamber was kept in desired temperature for more than 12 h before the cold-start in order to ensure that all parts of the cell were in the same temperature. After that, the hydrogen flow was set on and the cell was operated at the open circuit state for 3 min after the open circuit potential achieved its typical value of approximately 0.95 V. The average current density was increased from 0 to 200 mA cm<sup>-2</sup> at -5 °C and from 0 to 300 mA cm<sup>-2</sup> at -10 °C in steps of 0.1 A. The intervals between the current steps were 30 and 60 s. After cold-start the cell was operated ca. 4 h at the desired current density level. Polarization measurements were also conducted between cold-start measurements in order to see possible irreversible changes in the performance.

### 3. Results

#### 3.1. Effect of subzero temperatures

The cell voltage and resistance as a function of time from the measurement at chamber temperature of 0 °C are illustrated in Fig. 2a, and measured chamber and cell temperatures in Fig. 2b. The chamber temperature ( $T_{\text{ch}}$ ) stabilized to the desired value in ca. 1 h. The cell temperatures measured from

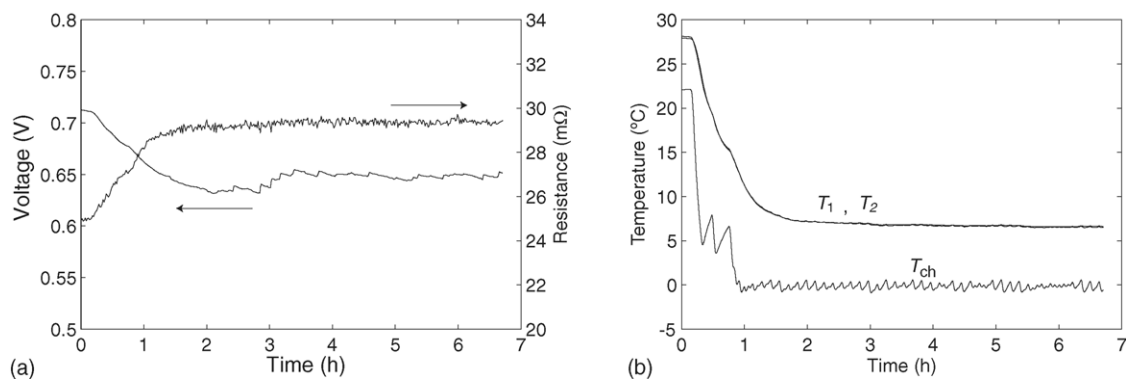


Fig. 2. Results from the measurement  $T_{\text{ch}} = 0$  °C: (a) voltage and resistance curves and (b) chamber and cell temperatures.

the cathode surface decreased asymptotically towards  $6.6^{\circ}\text{C}$  ( $T_1$  and  $T_2$ ). The fluctuation in cell temperatures was less than  $\pm 0.05^{\circ}\text{C}$  and the cell temperatures were the same within the tolerance of the temperature probes, which was  $0.15^{\circ}\text{C}$ . The cell voltage decreased simultaneously with the temperature and reached a stable value of approximately  $0.65\text{ V}$ , which was  $60\text{ mV}$  less than the initial value.

The decrease in the cell performance was due to increased cell resistance, increased activation overpotential, and possibly also increased mass diffusion overpotential. The increase in the cell resistance was most probably due to decreased protonic conductivity of the membrane. The increase in activation overpotential is due to decelerated electrode reactions at lower temperatures. The increase in mass diffusion overpotential is caused by increased liquid water saturation, as the saturation pressure of water vapor is significantly decreased at lower temperatures. The absolute increase in the measured cell resistance would suggest a voltage drop of approximately  $5\text{ mV}$ , which is significantly less than was observed. In addition, there was very little liquid water observed at the surface of the cathode GDB implying only small increase in mass diffusion overpotential. Thus it seems that the main contributor to the performance loss is the decelerated reaction rates. The measurement of the polarization curve after the measurement at  $0^{\circ}\text{C}$  showed no irreversible changes in the cell performance.

The results from the measurement at chamber temperature of  $-5^{\circ}\text{C}$  are not illustrated here because the results were very similar to the ones presented in Fig. 2. The stable cell voltage was slightly decreased and resistance increased compared to the performance at  $0^{\circ}\text{C}$ , and the values were approximately  $0.64\text{ V}$  and  $30.1\text{ m}\Omega$ , respectively. The chamber temperature stabilized to  $-5^{\circ}\text{C}$  ca. in 1 h, and the cell temperatures decreased towards  $2.0^{\circ}\text{C}$ . There were no irreversible changes in the cell performance observed in the polarization scan after the measurement.

At  $-10^{\circ}\text{C}$  with the current density of  $300\text{ mA cm}^{-2}$  the operation of the cell was similar to the previous measurements. The cell voltage stabilized to approximately  $0.58\text{ V}$  and resistance to  $30.3\text{ m}\Omega$ . The chamber temperature stabilized to  $-10^{\circ}\text{C}$  in 1.5 h and the cell temperature  $T_1$  decreased down to  $0.7^{\circ}\text{C}$ . The cell temperature  $T_2$  started to deviate from  $T_1$  after 7 h as the product water started to accumulate on the lower part of the cell and also on the top of the sensor. The ice formation after 12 h of measurement is illustrated in Fig. 3a.  $T_2$  was approximately  $0.3^{\circ}\text{C}$  after 12 h of measurement and it had a fluctuation of  $\pm 0.1^{\circ}\text{C}$  with a 10 min time-scale. Irreversible performance losses were not observed in the polarization scan after the measurement.

The results from the measurement at  $-10^{\circ}\text{C}$  with the current density of  $200\text{ mA cm}^{-2}$  are illustrated in Fig. 4. It seems that in this measurement the heat production of the cell was not high enough to prevent some of the product water from freezing inside the cell. The cell voltage started to decrease after 4 h and stabilized to approximately  $0.45\text{ V}$  with a significant fluctuation. The cell resistance was simultaneously increased. The voltage fluctuation has an apparent pattern with a time-scale of ca. 30 min, which may be due to some kind of freezing–melting cycle of product water inside the cell. When freezing of product water occurs, the voltage is decreased and thus the heat production is simultaneously increased causing the frozen water to melt. Both of the cell surface temperatures fell below  $0^{\circ}\text{C}$  in 1.5 h and had a slight increase after 4 h as the heat production is increased due to decrease in cell voltage. The accumulated product water froze on the lower parts of the cell, but not above the active area as shown in Fig. 3b. The fluctuation of  $T_2$  was due to ice formation on the top of the sensor.

When using dry hydrogen it is evident that some of the produced water is transported through the membrane to the anode. When the hydrogen outlet is at a temperature below the freezing point of water, it is possible that the outlet will

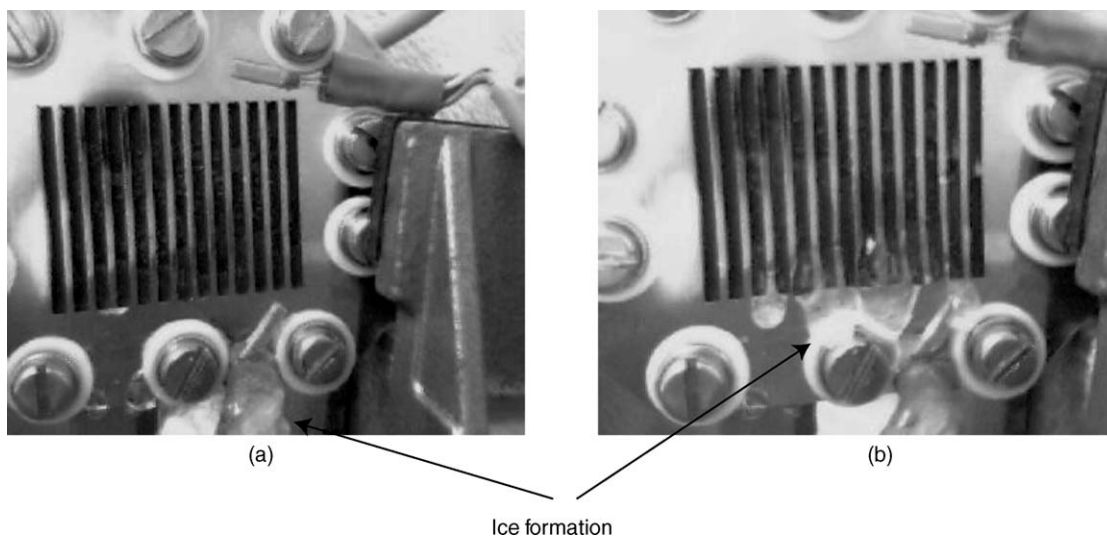


Fig. 3. Ice formation on the lower parts of the cell at  $T_{\text{ch}} = -10^{\circ}\text{C}$ : (a)  $i = 300\text{ mA cm}^{-2}$ , image taken after 12 h and (b)  $i = 200\text{ mA cm}^{-2}$ , image taken after 8 h.

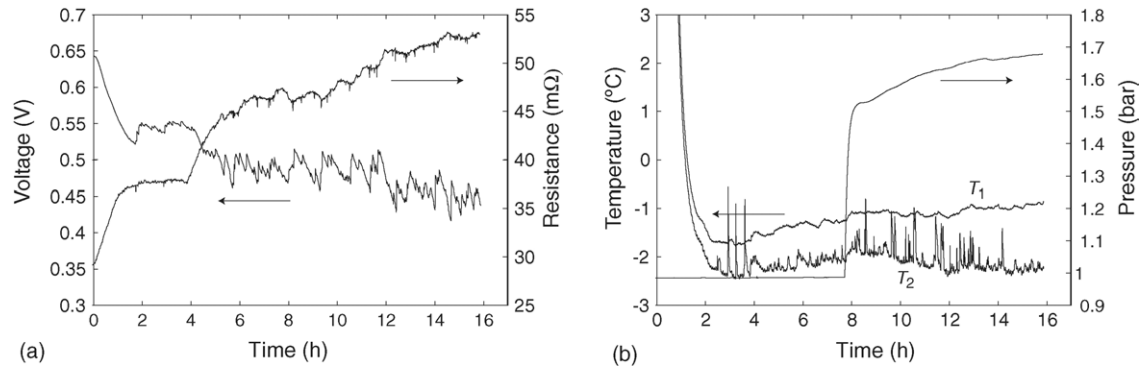


Fig. 4. Results from the measurement  $T_{\text{ch}} = -10\text{ }^{\circ}\text{C}$  and  $i = 200\text{ mA cm}^{-2}$ : (a) voltage and resistance curves and (b) cell temperatures and hydrogen pressure.

freeze. This was observed in this measurement as the hydrogen outlet was blocked by ice after 8 h causing an increase in hydrogen pressure. The pressure increased quite fast to 1.5 bar after which it slowly increased up to 1.7 bar implying that the hydrogen leaked through the anode gaskets and possibly also directly through the membrane. A slight increase in resistance with the increase in hydrogen pressure can be observed in Fig. 4. It is possible that increased hydrogen crossover simultaneously increases water flux from the anode to cathode thus increasing resistance. Even though the results imply that some freezing of the product water occurred inside the cell, no irreversible performance losses observed in the polarization scan after the measurement.

The results from the measurement at  $-15\text{ }^{\circ}\text{C}$  with the current density of  $300\text{ mA cm}^{-2}$  are illustrated in Fig. 5. The cell voltage was rather unstable throughout the measurement and on the average decreased monotonically after 4 h due to ice formation. Both of the cell temperatures decreased below  $0\text{ }^{\circ}\text{C}$  in an hour. The heat production in this measurement was not sufficient to prevent the ice formation also on the surface above the active area. After 2 h, the cell resistance increased significantly, which was possibly caused by the internal icing of the cell. At the end of the measurement over one third of the surface above the active area of the cell was covered with ice as illustrated in Fig. 9a. The hydrogen outlet was blocked by ice after 6 h and the pressure increased rapidly to 1.5 bar after which it was slowly increased to 1.6 bar. Interestingly,

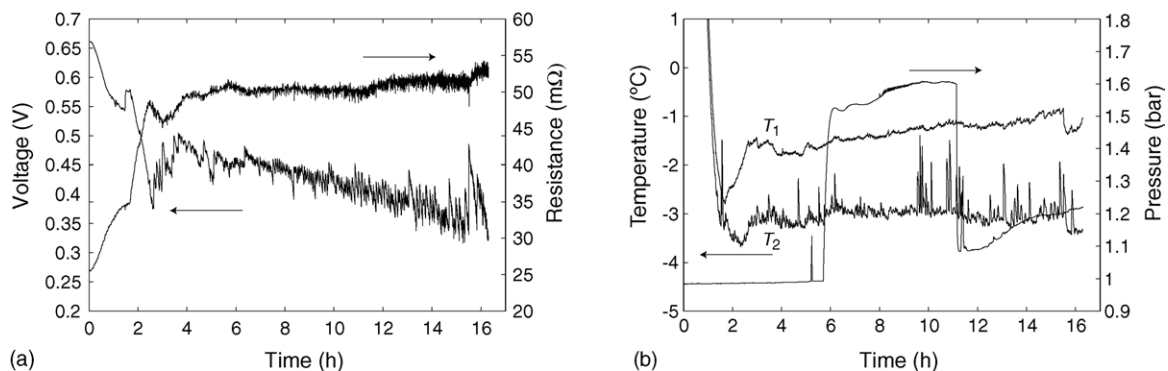


Fig. 5. Results from the measurement  $T_{\text{ch}} = -15\text{ }^{\circ}\text{C}$  and  $i = 300\text{ mA cm}^{-2}$ : (a) voltage and resistance curves and (b) cell temperatures and hydrogen pressure.

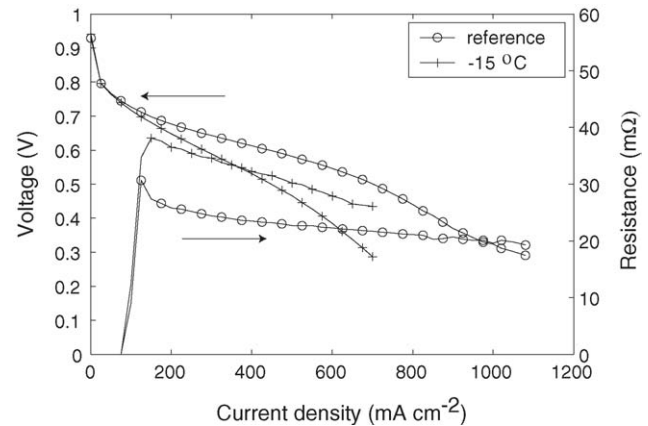


Fig. 6. Reference polarization and resistance curves and the ones measured after the measurement at  $-15\text{ }^{\circ}\text{C}$  with the current density of  $300\text{ mA cm}^{-2}$ . Every other measurement point marker is removed in order to make the figure clearer.

the pressure decreased after 11 h to 1.1 bars indicating a hydrogen leakage.

The freezing of product water in this measurement was so serious that an irreversible performance loss was observed. This can be seen from the measured polarization and resistance curves, which are illustrated in Fig. 6 with a reference curve. The performance loss is quite significant; e.g. the difference in the cell voltage at  $700\text{ mA cm}^{-2}$  is over 200 mV. It

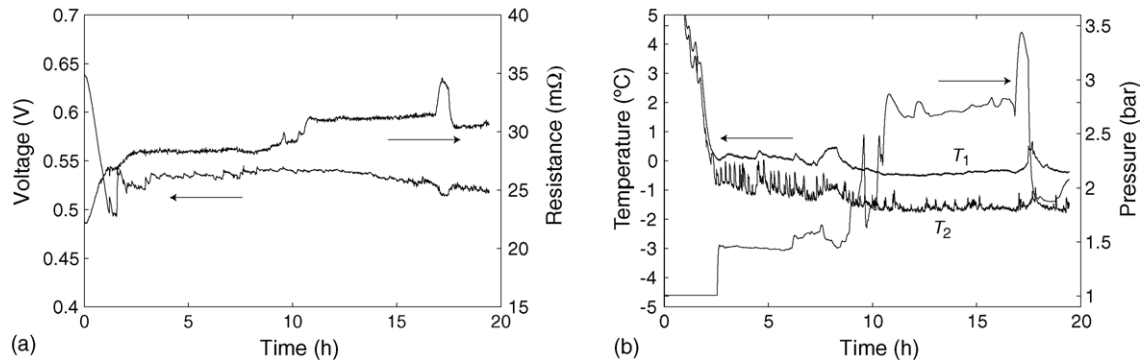


Fig. 7. Results from the measurement  $T_{ch} = -15\text{ °C}$  and  $i = 400\text{ mA cm}^{-2}$ : (a) voltage and resistance curves and (b) cell temperatures and hydrogen pressure.

seems that the product water was frozen also inside the cell because the resistance and mass diffusion overpotential increased. The increase in resistance may be due to irreversible structural changes in bulk materials caused by volumetric expansion of water during congelment. Partial detachment of different components from each other because of ice formation at the boundaries between them is also possible, causing higher contact resistance. The increased mass diffusion overpotential may be due to irreversible pore size changes inside the electrode and gas diffusion backing.

At  $-15\text{ °C}$  with the current density of  $400\text{ mA cm}^{-2}$  the operation of the cell was quite stable as can be seen from the measurement results illustrated in Fig. 7. The cell voltage stabilized to approximately 0.54 V and showed a very slight decrease towards the end of the measurement. Cell temperature  $T_1$  was slightly above  $0\text{ °C}$  and after 9 h it fell slightly below  $0\text{ °C}$ . There was very little ice formation and also some liquid water on the surface of lower parts of the cell. The hydrogen outlet was blocked by ice after 2.5 h and the hydrogen pressure was increased to ca. 1.5 bar. After 6 h the pressure started to fluctuate and achieved a maximum of 3.4 bar. It is possible that some of the product water froze between the gaskets improving the gas tightness until the pressure was high enough to remove the blockage. It is worth noting that the cell resistance follows the hydrogen pressure. This observation supports the assumption that possible increase in

hydrogen leakage through the membrane increases also the water flux decreasing the protonic conductivity. The polarization curve showed no irreversible performance losses after the measurement implying that the cell is capable of managing noticeable pressure differences over the membrane at least for some periods of time.

At  $-20\text{ °C}$  with the current density of  $500\text{ mA cm}^{-2}$  the operation of the cell was very similar to that in the previous measurement. The cell voltage stabilized to approximately 0.48 V and showed a slight decrease towards the end of the measurement. Cell temperature  $T_1$  decreased to ca.  $-1.3$  to  $-0.7\text{ °C}$  and  $T_2$  to  $-2.5\text{ °C}$  with a fluctuation of  $\pm 0.4\text{ °C}$ . There was significant amount of ice on the surface of the lower part of the cell but not above the active area. The hydrogen outlet was blocked by ice in 1.5 h and hydrogen pressure was increased to 1.5 bar. Hydrogen pressure started to fluctuate after 6 h similarly to previous measurement achieving a maximum of 3.7 bar. The cell resistance followed again the hydrogen pressure. There were no irreversible changes in the cell performance observed in the polarization curve after the measurement.

The results from the measurement at  $-27.5\text{ °C}$  are illustrated in Fig. 8. Pressure data was not available from this measurement because of a data collection error. The chamber temperature reached  $-26\text{ °C}$  in 2.5 h and decreased asymptotically towards the target value, which was reached in 7 h.

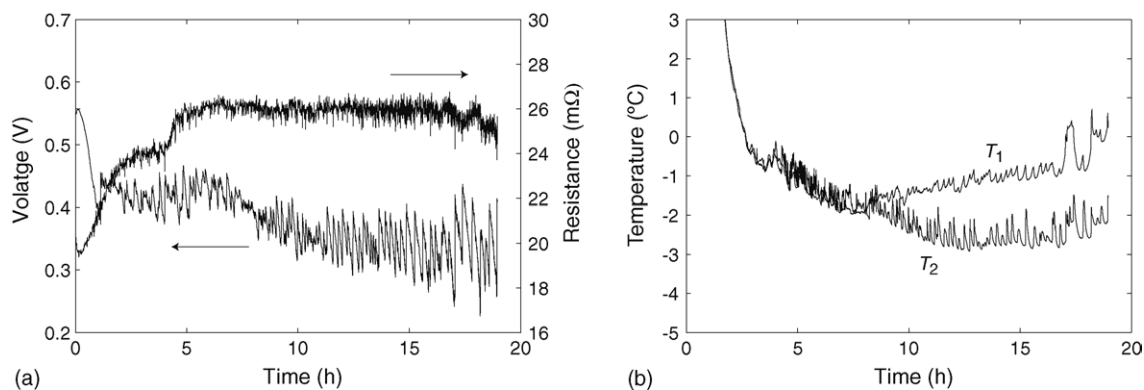


Fig. 8. Results from the measurement  $T_{ch} = -27.5\text{ °C}$  and  $i = 600\text{ mA cm}^{-2}$ : (a) voltage and resistance curves and (b) cell temperatures.

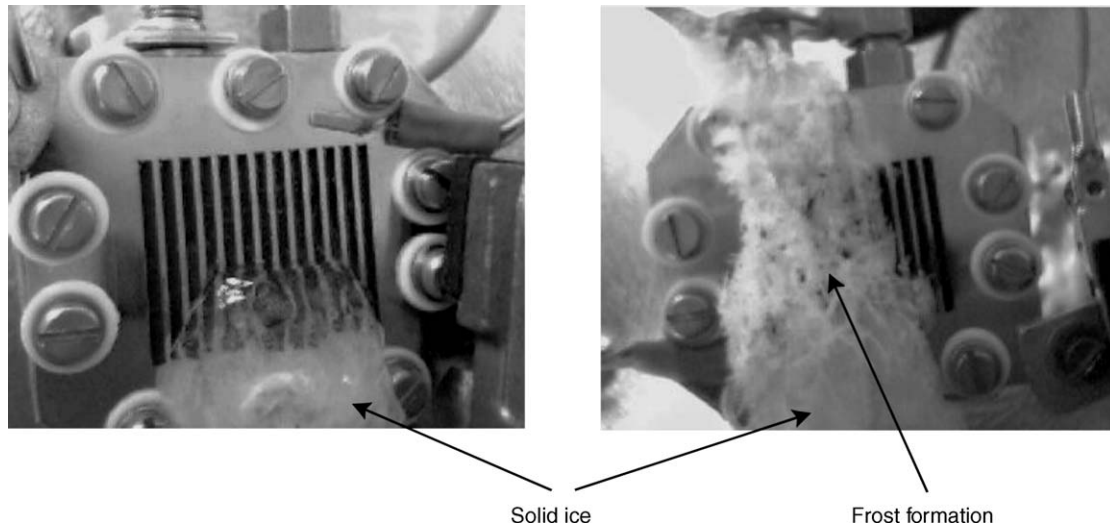


Fig. 9. (a) Ice formation on the lower parts of the cell at  $T_{\text{ch}} = -15\text{ }^{\circ}\text{C}$  and  $i = 300\text{ mA cm}^{-2}$  and (b) frost formation due to irreversible sublimation of product water at  $T_{\text{ch}} = -27.5\text{ }^{\circ}\text{C}$ .

The cell voltage decreased to an average value of approximately 0.41 V with a fluctuation of  $\pm 30\text{ mV}$ . After 8 h the average cell voltage started to slowly decrease and the fluctuation increased being  $\pm 60\text{ mV}$  at the end of the measurement. The decrease in cell voltage and increase in fluctuation was most probably due to ice formation causing additional mass diffusion overpotential. Reversible sublimation of product water was observed during the measurement, as frost was formed above the active area as illustrated in Fig. 9b. The frost formation was attached to the upper and lower parts of the cell and there was an air space of several millimeters on the sides of the formation and above the active area. The formation most probably decreased mass transfer by disturbing the free-convection occurring on the surface of the cell, but it was very porous and fragile, and thus there was a path for oxygen supply to the cell both through the formation and from the open sides of it. After the measurement the frost formation collapsed from a little touch and there was a block of solid ice only on the lower part of the cell similarly to the one illustrated in Fig. 9a, but the block was smaller and practically not above the active area.

### 3.2. Cold-start measurements

The cold-start behavior of the cell at  $-5\text{ }^{\circ}\text{C}$  is illustrated in Fig. 10a and at  $-10\text{ }^{\circ}\text{C}$  in Fig. 10b. The cell was capable of starting operation at  $-5\text{ }^{\circ}\text{C}$  without any difficulties. At  $-10\text{ }^{\circ}\text{C}$  the cell was capable of starting operation with the slower starting procedure, i.e., with 60 s intervals between current steps. With the faster procedure at  $-10\text{ }^{\circ}\text{C}$  the cell operated without problems up to  $233\text{ mA cm}^{-2}$ , but after trying to further increase the current the cell voltage collapsed and the current was turned off. Most probably, the cell did not heat rapidly enough with the faster starting procedure in order to prevent fatal freezing of the product water inside the cell. The chamber was opened and the cell was let to warm up to ambient temperature directly after the unsuccessful cold-start.

The polarization and resistance curves before and after the cold-start measurements are illustrated in Fig. 11. There is no significant difference in the polarization curves after the cold-start measurements at  $-5\text{ }^{\circ}\text{C}$  implying that the product water did not freeze inside the cell. Even though the cell was capable

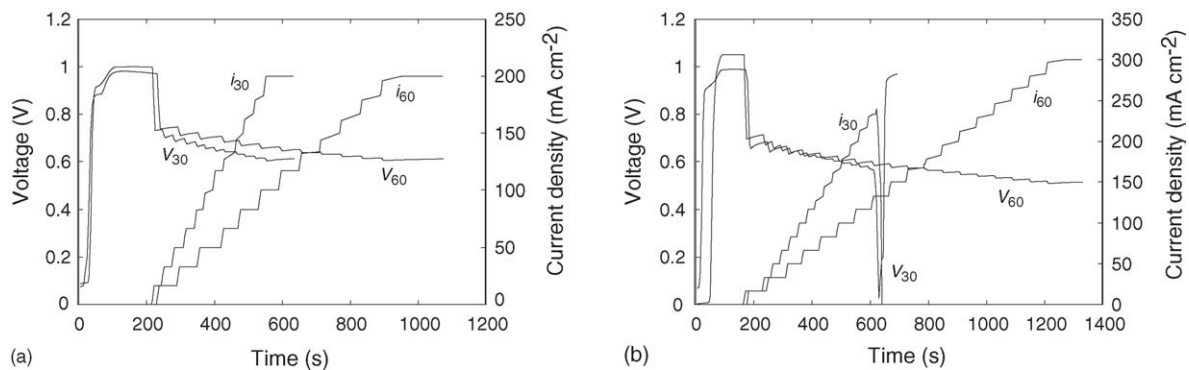


Fig. 10. Cold-start behavior of the cell: (a)  $T_{\text{ch}} = -5\text{ }^{\circ}\text{C}$  and (b)  $T_{\text{ch}} = -10\text{ }^{\circ}\text{C}$ . The notation (V for voltage and  $i$  for current density) next to curves tells the time between current steps in different starting procedures.

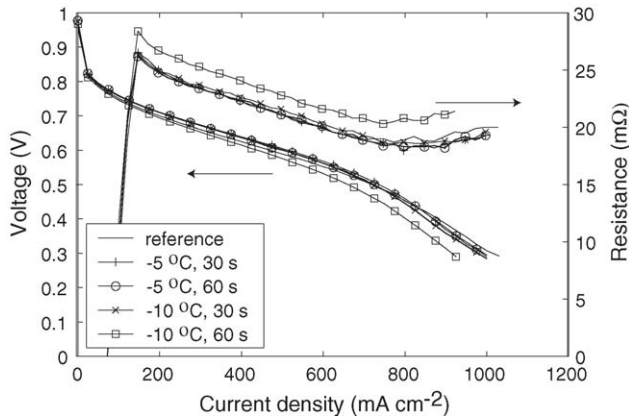


Fig. 11. Polarization and resistance curves of the cell before and after the cold-start measurements. Notations in the legend tell after which cold-start the corresponding curves were measured. Notation 'reference' refers to the measurement conducted before cold-starts. Every other measurement point marker is removed in order to make the figure clearer.

of starting operation with the slower procedure at  $-10^{\circ}\text{C}$ , the measured curves show a slight increase in mass diffusion overpotential and resistance implying that there was some freezing occurred inside the cell causing irreversible structural changes. Interestingly, there is no apparent change in the performance after the unsuccessful cold-start at  $-10^{\circ}\text{C}$ . This may be due to the fact that the cell was operated quite a short time at small current density, and thus the amount of produced water was also small. The cell was let to warm up immediately after the cold-start, and even though it seems that freezing of product water occurred, the amount of formed ice was small enough in order not to cause any irreversible changes.

The cell voltage and temperature curves from the successful cold-start measurements are illustrated in Fig. 12. Only upper cell temperature ( $T_1$ ) data is shown in Fig. 12 because the cell temperatures were practically identical. The cell voltage and temperature after the cold-start at  $-5^{\circ}\text{C}$  stabilized to practically same level as in constant current measurement at corresponding time. The stabilized temperature level was the

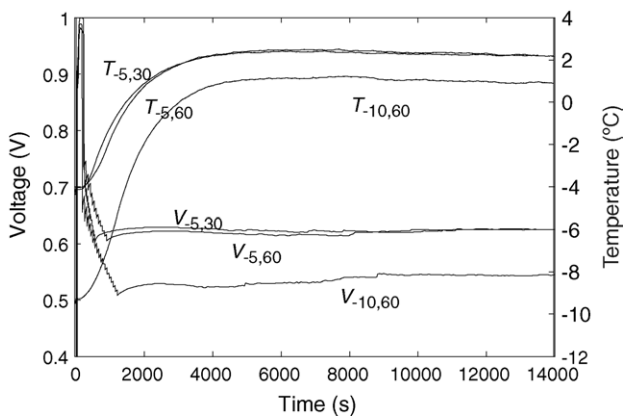


Fig. 12. The cell voltage and temperature after the cold-starts. The notation tells from which measurement the corresponding curve is.

same also after the cold-start at  $-10^{\circ}\text{C}$ , but the voltage was approximately 30 mV lower. This performance loss supports the assumption of freezing of product water inside the cell.

#### 4. Summary and discussion

The effect of subzero temperatures on the performance of planar free-breathing PEMFC was studied by placing the cell into a temperature chamber. The performance was studied with constant current measurements at temperatures between 0 and  $-27.5^{\circ}\text{C}$  and with cold-start measurements at  $-5$  and  $-10^{\circ}\text{C}$ .

Constant current measurements showed that the cell was able to operate at cold temperatures if the current density, and thus also the heat production, was high enough in order to avoid internal freezing of the cell. Cell voltage was stable in these measurements, but it was significantly lower than the initial level because of different loss mechanisms. The main reason for decreased cell voltage seemed to be the increased activation overpotential due to decelerated reaction rates. At the lower temperatures the cell voltage fluctuated and showed also a slight decrease towards the end of the measurement. In case where the heat production was too small, irreversible performance losses occurred due to structural changes of the cell components.

Significant ice formation was noticed at the lower parts of the cell at lower temperatures. In most of the measurements the ice was formed mainly above inactive areas, but at chamber temperature of  $-15^{\circ}\text{C}$  with  $300\text{ mA cm}^{-2}$  current density, there was ice formation also partly above the active area due to inadequate heat production. When the temperature of the chamber was  $-27.5^{\circ}\text{C}$ , reversible sublimation of water was observed and the active area of the cell was partly covered with highly porous frost. The reversible sublimation of water, i.e. the direct phase change from water vapor into ice, is possible when the water vapor temperature is below the triple point temperature ( $0.01^{\circ}\text{C}$ ) and partial pressure of water vapor is low enough (less than 611 Pa). It seems that the convection was enhanced with the high temperature difference between the cell and ambient air at chamber temperature of  $-27.5^{\circ}\text{C}$ , being able to remove water from the cell surface effectively enough in order to decrease the partial pressure below the triple point and thus enabling the observed reversible sublimation.

Hydrogen exhaust froze at low chamber temperatures and the cell started to operate in the dead-end mode. In these measurements the hydrogen inlet pressure increased and a pressure gradient was formed over the cell. The cell was able to operate even with a 2.4 bar pressure difference. It was observed that the cell resistance followed the pressure difference. This was possibly caused by an increase in water transport from the anode to cathode when the hydrogen pressure was increased. The increased water transport decreased the humidity of the membrane at the anode side and thus increased the resistance.



The cold-start measurements showed that the initially dry cell was able to start at  $-5^{\circ}\text{C}$  without any difficulties when the current was increased with 0.1 A steps with 30 and 60 s intervals. At  $-10^{\circ}\text{C}$  with the faster current increase rate the cell operated well up to  $233\text{ mA cm}^{-2}$  current density, after which the cell voltage collapsed. This was probably caused by freezing of the product water inside the cell. When the current increase rate was decreased to 60 s intervals, the cell started without any problems at  $-10^{\circ}\text{C}$ . However, there was a slight irreversible performance loss observed after this cold-start implying that some internal freezing of the cell had occurred.

The main results of this paper are presented in the bullet list below. It should be pointed out that these results are valid only for this certain cell type, and thus one should use caution in generalization of these results.

- Planar free-breathing PEMFC is able to operate at cold temperatures presuming that the heat production is high enough.
- Irreversible performance losses are encountered if the product water freezes inside the cell.
- The cell is able to perform a cold-start down to  $-10^{\circ}\text{C}$ , but problems may be encountered below  $-5^{\circ}\text{C}$ .
- The cell is able to operate in a dead-end mode with pressurized anode.

## References

- [1] T. Hottinen, M. Noponen, T. Mennola, O. Himanen, M. Mikkola, P. Lund, *J. Appl. Electrochem.* 33 (2003) 265–271.
- [2] T. Hottinen, O. Himanen, P. Lund, K. Åström, ‘High power density thin PEMFC for portable applications’, Extended abstract, Fuel Cell Seminar, San Antonio, USA, 2004.
- [3] E.A. Cho, J.-J. Ko, H.Y. Ha, S.-A. Hong, K.-Y. Lee, T.-W. Lim, I.-H. Oh, *J. Electrochem. Soc.* 150 (2003) 1667–1670.
- [4] E.A. Cho, J.-J. Ko, H.Y. Ha, S.-A. Hong, K.-Y. Lee, T.-W. Lim, I.-H. Oh, *J. Electrochem. Soc.* 151 (2004) 661–665.
- [5] Y. Hishinuma, T. Chikahisa, F. Kagami, T. Ogawa, *JSME Int. J. Series B: Fluids Thermal Eng.* 47 (2004) 235–241.
- [6] B.K. Datta, G. Velayutham, A.P. Goud, *J. Power Sources* 106 (2002) 370–376.
- [7] T. Hottinen, O. Himanen, P. Lund, *J. Power Sources* 138 (2004) 205–210.
- [8] T. Hottinen, M. Mikkola, T. Mennola, P. Lund, *J. Power Sources* 118 (2003) 183–188.